A Volcano Rekindled: The Renewed Eruption of Mount St. Helens, 2004–2006
Edited by David R. Sherrod, William E. Scott, and Peter H. Stauffer
U.S. Geological Survey Professional Paper 1750, 2008

Chapter 20

Frictional Properties of the Mount St. Helens Gouge

By Peter L. Moore[1], Neal R. Iverson[1], and Richard M. Iverson[2]

Abstract

Frictional properties of gouge bounding the solid dacite plug that extruded at Mount St. Helens during 2004 and 2005 may have caused stick-slip upward motion of the plug and associated seismicity. Laboratory experiments were performed with a ring-shear device to test the dependence of the peak and steady-state frictional strength of the gouge on shearing rate and hold time. A remolded gouge specimen (~0.012 m^3) was sheared under constant normal stresses ranging from 5 to 200 kPa and at rates ranging from 10^{-6} to 10^{-3} m/s. The gouge exhibited rate-weakening behavior at rates lower than 1×10^{-4} m/s and rate-strengthening at rates above 5×10^{-4} m/s. Peak strengths occurred during the onset of shearing, when displacements were generally less than 0.5 mm. In slide-hold-slide tests, the peak strength of the gouge increased logarithmically as hold times increased from 3 s to almost 10^5 s.

Rate-weakening friction is a requirement for stick-slip behavior that is satisfied by the Mount St. Helens gouge. Indeed, regular stick-slip oscillations were observed in two experiments performed at the highest normal stress and lowest rates of shear. The conditions under which this stick-slip motion occurred indicate that the gouge also satisfies a second criterion for stick-slip behavior of materials exhibiting rate-and-state dependent friction—gouge stiffness exceeds that of the ascending magma that drives upward motion of the plug. The presence of highly compliant magma as a driving element may be crucial for generating stick-slip instabilities at the shallow earthquake focal depths observed during the eruption.

Introduction

Lava dome formation during the 2004–2005 eruption of Mount St. Helens was accompanied by abundant, nearly periodic, shallow-focus earthquakes. These "drumbeat" earthquakes had magnitudes <2, focal depths <1 km, and they typically recurred about every 1–2 minutes. This seismicity is thought to have resulted from incremental uplift of a solid dacite plug driven by magma ascent from below at rates of roughly 1–2 m^3/s (Iverson and others, 2006). Wear along the margin of the plug produced a layer of crushed rock, or gouge, of the same lithology as the extruding rock (fig. 1). Observed at the surface, this gouge formed a coating 0.1–1 m thick on freshly exposed faces of the lava dome. Moreover, these freshly exposed faces were conspicuously striated in directions mostly parallel to the direction of plug motion, indicating that gouge deformation probably accommodated much of the upward displacement of the plug mass. Interpretation of the source of drumbeat seismicity, therefore, requires knowledge of the frictional properties of this gouge.

Gouge is generated by the wear and cataclasis of rock during frictional shear and develops progressively with shear displacement (for example, Engelder, 1974). Although cataclasis may occur episodically in rapidly strained magma near its solidus (for example, Tuffen and Dingwell, 2005), granular gouge dredged from the margin of the new Mount St. Helens lava dome early in 2005 was cool, noncohesive, and bore evidence primarily of mechanical wear and comminution. Therefore, the frictional behavior of the gouge is likely similar to that of low-temperature gouge in shallow crustal faults. Consequently, frictional behavior observed in room-temperature laboratory experiments is relevant to interpreting dome extrusion processes during the 2004–2005 eruption of Mount St. Helens.

Theoretical Background

Rate- and State-Dependent Friction

Gouge behavior closely approximates that of a Coulomb material, such that its shear strength τ is described by $\tau = \mu\sigma'_n + c$, where σ'_n is the effective normal stress, c is cohe-

[1] Department of Geological and Atmospheric Sciences, Iowa State University, Ames, IA 50011

[2] U.S. Geological Survey, 1300 SE Cardinal Court, Vancouver, WA 98683

sion and μ is the coefficient of friction. In most granular media at low temperatures, μ can be considered nearly constant, but laboratory experiments have routinely shown that μ is slightly sensitive to both shear rate and the history of deformation. These deviations from a constant coefficient of friction are small but of great interest because under the appropriate conditions they give rise to an instability that may be responsible for earthquakes. In fault mechanics literature, these shear-rate and deformation-history effects are termed "rate" and "state" dependencies, respectively (see Marone, 1998, for a review).

Stemming from the work of Dieterich (1979) and Ruina (1983), the most common expression of the rate- and state-dependence of friction is

$$\mu = \mu_0 + a\ln\left(\frac{V}{V_0}\right) + b\ln\left(\frac{\theta V_0}{D_c}\right), \qquad (1)$$

where μ_0 is a reference coefficient of friction applicable at a reference shear displacement rate V_0, V is shear displacement rate (with dimensions of length/time), θ is a state variable (with dimensions of time), D_c is a characteristic slip distance over which friction adjusts to a steady state in response to a velocity change, and a and b are positive coefficients that are typically of order 10^{-3} to 10^{-2}. Individually, the parameters a and b describe the relative magnitude of the so-called "direct" and "evolution" effects, respectively. The direct effect is a near-instantaneous response of friction to a change in shear rate, whereas the evolution effect is a transient response that takes place over the characteristic length scale D_c. Note that in this paper, we use the term "shear rate" to denote shear displacement rates such as V. Where we wish to distinguish such rates from shear strain rates, which have dimensions of inverse time, we do so explicitly.

The state variable θ in equation 1 describes a time-dependent effect that can be viewed as the length of time that a set of grain contacts persists at a given velocity (Scholz, 2002). According to Dieterich (1979), the evolution of θ with time may be described by

$$\frac{d\theta}{dt} = 1 - \left(\frac{V\theta}{D_c}\right). \qquad (2)$$

Although the characteristic slip distance can be determined from stress-displacement data from experiments with bare rock, it is difficult to determine in experiments with gouge because this displacement depends on the strain distribution in the gouge (Marone and Kilgore, 1993). In a steady state ($d\theta/dt = 0$), $\theta = D_c/V$ and equation 1 reduces to

$$\mu_{ss} = \mu_0 + (a - b)\ln\left(\frac{V}{V_0}\right), \qquad (3)$$

where μ_{ss} is the steady-state friction coefficient. The sensitivity of steady-state frictional strength to shear rate, therefore, is given by the difference between the coefficients a and b for the direct and evolution effects:

$$a - b = \frac{\mu_{ss} - \mu_0}{\ln(V/V_0)}. \qquad (4)$$

If this difference is negative, the material weakens with increasing slip rate, and conversely, if $a - b$ is positive, the material strengthens with increasing slip rate (Scholz, 2002). The coefficients a and b are usually determined experimentally by conducting velocity-stepping triaxial or direct-shear experi-

Figure 1. Photograph of striated gouge near base of extruding spine at Mount St. Helens, July 28, 2005. Field of view approximately 20 m.
USGS photo by S.P. Schilling.

ments in which shear rate is varied over a wide range during continuous shear.

Consistent with Dieterich's original reasoning (Dieterich, 1972, 1978, 1979), Beeler and others (1994) demonstrated that the parameter b can also be determined independently by measuring the variation in peak friction as a function of the time that shear is stopped ("hold time"), such that

$$b = \frac{d\mu_{\text{peak}}}{d\ln(t_{\text{hold}})} \quad . \qquad (5)$$

Peak shear strength typically increases logarithmically with time as sliding surfaces are held in stationary contact. The mechanisms responsible for this aging effect are thought to be associated with compaction and growth of the area of solid-to-solid grain contact across the shear zone (Losert and others, 2000; Scholz, 2002).

Relation Between Gouge Frictional Behavior and Seismicity

If gouge becomes weaker as shear rate increases ($a - b < 0$), slip instability and stick-slip motion are possible, but according to the rate-and-state dependent friction model, rate weakening alone is not sufficient to induce stick-slip behavior (Rice and Ruina, 1983; Ruina, 1983). The stiffnesses of the gouge and the system that loads the gouge are also important. The decline from peak (static) frictional strength to steady-state (dynamic) strength of the gouge requires a finite displacement that exceeds but is proportional to the characteristic slip distance, D_c. If elastic strain in the materials loading the shear zone is relaxed over a displacement larger than D_c, the applied driving stress momentarily exceeds the resisting stress and slip accelerates until driving and resisting stresses become equal (fig. 2). As defined by Ruina (1983), the "critical stiffness" of the gouge, k_{crit}, is the ratio of shearing-resistance decline to characteristic slip distance upon a change in slip velocity, and k_{crit} has dimensions of stress per unit length. If the loading system requires a slip distance much greater than D_c to reduce the applied stress from the peak to steady-state strength, the loading system's stiffness is smaller than k_c and stick-slip behavior is possible (fig. 2).

According to the arguments summarized above, repetitive stick-slip motion along the subsurface margins of the extruding dacite plug at Mount St. Helens can occur if two conditions are met—(1) the gouge must exhibit rate-weakening behavior at the imposed loading rate, and (2) the most compliant component of the loading system (that is, the magma) must have a stiffness smaller than the critical stiffness of the gouge. The first requirement is readily evaluated with our laboratory experiments. The second requirement is more difficult to address, but our experiments and inferences about the magma-plug system at Mount St. Helens provide some constraints.

Experimental Methods

Gouge was obtained by dredging the surface of the newly extruded spine at Mount St. Helens by helicopter in February 2005. Ring-shear tests were performed at room temperature with dry, remolded specimens. Particles with diameters larger than one-tenth the smallest dimension of the specimen chamber (70 mm) were removed from the gouge, consistent with normal geotechnical testing procedure (Head, 1989). Shearing rates and normal stresses were varied among tests through the ranges permitted by the device (5×10^{-3} to 1.5×10^{-6} m/s and 5 to 195 kPa respectively). These experiments differed from velocity-stepping tests (for example, Blanpied and others, 1987; Biegel and others 1989; Marone and others, 1990) in that shear-rate changes were made only after first stopping shear.

The ring-shear device (detailed in Iverson and others, 1997) has been used to study the mechanical properties of a variety of granular geological materials (for example, Iverson and others, 1998; Iverson and others, 2000; Moore and Iverson, 2002; Scherer and others, 2004). Its large capacity permits inclusion of larger particles that are common in gouge, but the test specimen's large surface area limits the magnitude

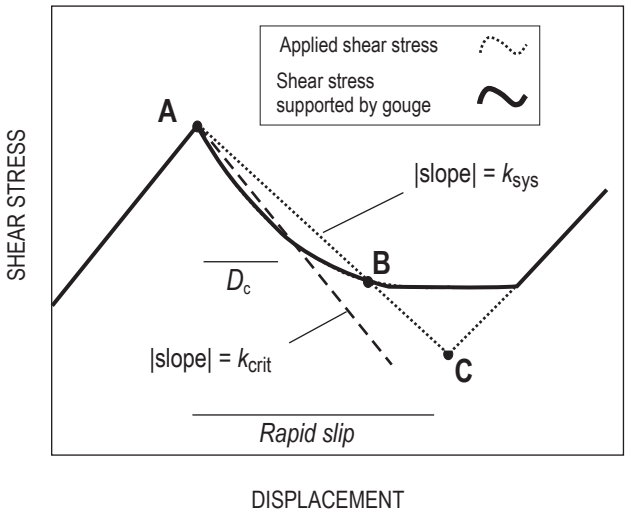

Figure 2. Stress applied by the loading system and shear stress supported by gouge during a stick-slip cycle. When slip commences at A, strength of the gouge initially declines more rapidly than the stress applied by the loading system, and acceleration occurs. When driving and resisting forces are equal again at B, slip begins to decelerate and stops at C. Slope of the decline in applied stress with displacement is the stiffness of the system (k_{sys}). When this stiffness is smaller than the critical stiffness of the gouge k_{crit} as defined by the shear stress decline and the gouge's characteristic slip distance D_c, the system is susceptible to stick-slip. D_c is the characteristic distance of exponential decay of gouge shearing resistance during rapid slip (after Scholz, 2002).

of the normal stress that can be applied. The ~70-mm-thick specimen rests in an annular chamber (annulus OD = 0.600 m, ID = 0.370 m) and is gripped at its base by a toothed platen (fig. 3). This platen is screwed to a base plate, and it and the lower walls bounding the specimen rotate. The toothed lid of the specimen chamber is prevented from rotating with the base by a pair of stationary, horizontally oriented load cells, causing the specimen to shear. The force exerted by the lid on these load cells is approximately the shear force supported by the specimen. Shear is focused in a lens-shaped zone that is 10–30 mm in thickness at the centerline of the specimen and is centered on the sliding interface between the upper and lower walls (fig. 3*B*) (for example, Hooyer and Iverson, 2000). A stress normal to the shearing direction is applied with a lever system that presses downward on the lid (fig. 3*A*). The lid is free to move vertically if the porosity of the specimen changes, and this vertical displacement is measured continuously with three equally spaced linear variable displacement transducers (LVDTs) that press on the perimeter of the lid.

Vertical and circumferential frictional forces between the gouge and the upper walls bounding the specimen are measured independently with a load cell and torque sensor, respectively, which are contained within a suspension called the "yoke" (fig. 3*A*). The yoke holds the upper walls stationary and is not coupled to the lid. The measured forces on the walls are used to correct both the normal stress applied to the shear zone, which is reduced by upward wall drag in a consolidating specimen, and the shear resistance on the lid, which is reduced due to circumferential drag between the specimen and walls. However, owing to extrusion of fine sediment along the interface between the upper and lower walls, a component of the measured circumferential wall force is due to friction between the upper and lower walls rather than between the upper wall and specimen. Thus, when applied normal stress is small, this friction represents an unknown fraction of the wall correction necessary to estimate the total resistance to shear. As a result, in experiments with the smallest applied normal stresses (5–23 kPa), uncertainty in the measured shear stresses and associated friction coefficients is large. Despite the uncertainty, these low-stress measurements are, nevertheless, included to qualitatively illustrate patterns that are available only from the low-stress tests.

Two variable-speed electric motors (1/17 and 1/2 hp) were used to turn the base and thereby shear the gouge specimen. Used in combination with either one or two gearboxes, these motors enabled two ranges of shear rate—1.5×10^{-6} –2.5×10^{-5} m/s and 5.0×10^{-4}–5.0×10^{-3} m/s. The higher-power motor coupled to a single gearbox allowed shearing at the higher range of rates, but this configuration could not deliver sufficient torque to shear the gouge under normal stresses greater than 23 kPa. When the smaller motor was used with both gearboxes normal stresses of as much as 200 kPa could be applied. At higher normal stresses this motor/gearbox configuration was not sufficient to turn the rotating base.

Two groups of experiments were conducted. In one group designed to investigate the rate dependence of gouge friction, shear was driven at a constant rate until shearing resistance became steady, usually after 1–10 mm of total centerline displacement. Shear was then stopped to adjust the motor speed and restarted under the same normal stress, but at a new rate, until shearing resistance again became steady. This process was repeated at multiple shearing rates, and whenever possible tests were repeated in sequences of increasing and decreasing shear rate. In a second group of experiments, periods of shear, which were terminated once shearing resistance became steady, were separated by intervals of hold (no shear) that ranged from 3 seconds to more than one day. In these experiments, shear rate and normal stress were held constant so that the effects of hold time on peak friction could be isolated.

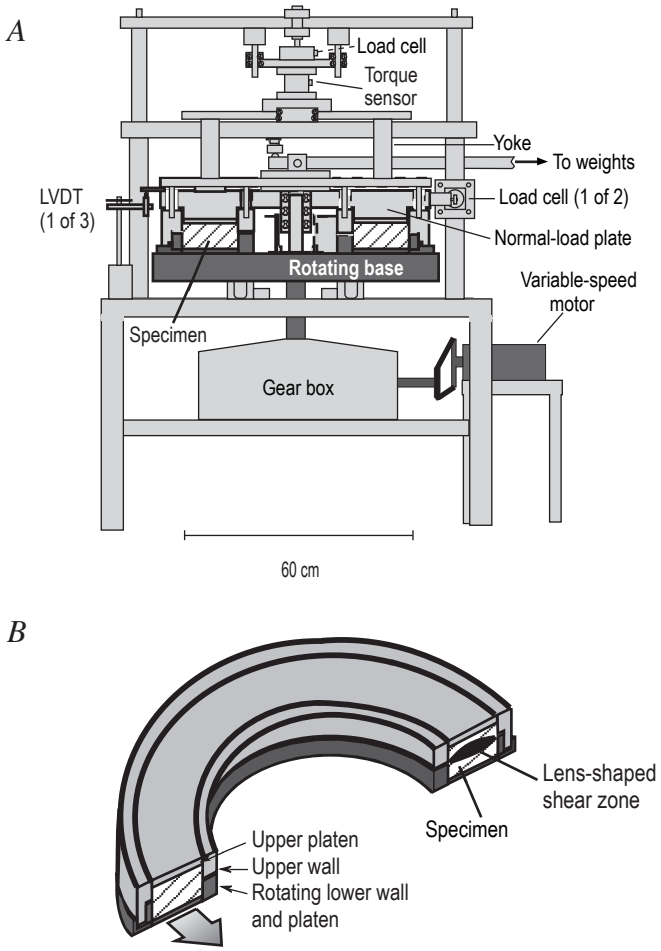

Figure 3. Ring-shear device. Gouge specimen is shown in cross-hachure. *A*, Diagrammatic cross section. Dark-gray parts rotate when motor is on. A second gearbox between motor and large gearbox was used in the experiments conducted at low shear rates (1.5×10^{-6} – 2.5×10^{-5} m/s). LVDT, linear variable displacement transducers. *B*, Oblique sketch of the specimen chamber. Shearing in gouge typically is focused in a lens-shaped zone, shown in black, centered on interface between stationary upper wall and rotating lower wall.

After some of the experiments, the gouge was sieved to measure whether there had been a size reduction of the largest grains; no size reduction could be detected indicating that little comminution or crushing occurred in the experiments.

Results

Data obtained in two typical ring-shear experiments, conducted at different shear rates under an applied normal stress of 159 kPa, are shown in figure 4. Following initial stress peaks related to the "direct effect" of changing shear rate, shear stress became approximately steady after displacements of less than 10 mm. The key feature illustrated by these two data series is that the steady-state shear strength of the gouge was smaller at the faster shear rate. For rates smaller than 10^{-4} m/s, such rate weakening was always observed, except for experiments conducted at a normal stress of 23 kPa in which the shear-rate dependence was neutral or slightly positive, depending on how the data are regressed (fig. 5). In the two sets of experiments conducted at faster shearing rates and low normal stresses, rate strengthening was observed (fig. 5*B*). Unfortunately, because of the torque limitations of our motor/gearbox configurations, the shear rate at which the transition to rate strengthening occurs cannot be pinpointed, but it appears to be on the order of 10^{-4} m/s for the range of stresses considered. As described previously, measurements at the lowest applied normal stresses are uncertain, but the consistently larger apparent friction coefficient at normal stresses of 5 kPa may indicate that the gouge has some cohesion. (Cohesion of about 1 kPa would decrease the apparent friction coefficient at 5 kPa to about 0.4 or 0.5, comparable to values measured at higher normal stresses.) Alternatively, the larger friction coefficient at 5 kPa may reflect steepening of the Coulomb failure envelope that is commonly observed at low normal stresses in various laboratory tests on granular materials (Lambe and Whitman, 1969).

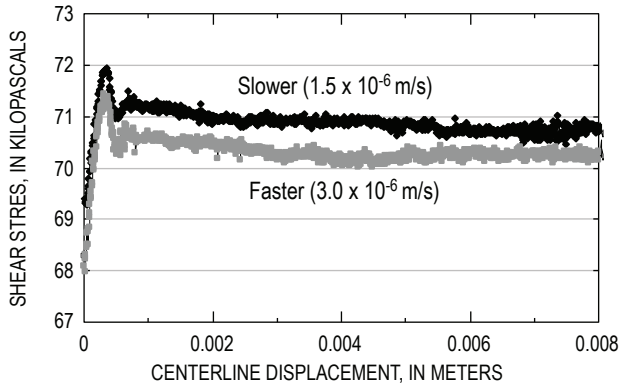

Figure 4. Stress-displacement data comparing two experiments conducted at normal stress of 159 kPa but at different shear rates. Prominent peaks in curves at ~0.5 mm of displacement are peak shear stresses, after which shear stress falls to steady-state value in both experiments.

Values of the rate-dependence parameter $a–b$ were estimated for each normal-stress level using equation 4 and a reference shear rate of 1.5×10^{-6} m/s, the smallest shear rate used in the experiments (table 1). Each value of $a–b$ was obtained from the slope of the linear regression of the steady-state friction coefficient against $\ln(V/V_0)$. Data from the "slow" (1.5×10^{-6} m/s to 2.5×10^{-5} m/s) and "fast" (5×10^{-4} m/s to 5×10^{-3} m/s) experiments were regressed separately. Values of $a–b$ at slow rates and high normal stresses (86–195 kPa) range from −0.0013 to −0.0103, indicating various degrees of rate weakening (fig. 5*A*).

In most of the ring-shear experiments, after a few millimeters of displacement, the shearing resistance of the gouge did not vary systematically, much as in the examples shown in figure 4. However, in the two experiments conducted at the largest normal stress and lowest shear rates, no steady shear stress developed. Instead, shear proceeded by regular stick-slip episodes (fig. 6). Major slip events were accompanied by abrupt consolidation, whereas dilation appeared to occur during "stick" intervals. Apparently the normal stresses and shear rates of these two experiments produced gouge stiffness and rate weakening that met both requirements for stick-slip behavior outlined previously.

In two sets of slide-hold-slide tests at a single shear rate and normal stress, peak strength increased logarithmically with hold time (fig. 7). Fitting these data to equation 5 indicates that $b = 0.0079$ (table 1). Hold time was also recorded during the variable-rate tests and, although these data have more scatter (perhaps due to a dependence of b on shear rate), they indicate a $b = 0.0075$. During hold periods compaction of the gouge was generally not observed, indicating either that growth of contact area between grains may not have been the key aging mechanism or that this effect was too subtle to be measured.

Discussion

Results of our ring-shear tests indicate that the Mount St. Helens gouge exhibits rate weakening at shear rates below about 10^{-4} m/s. At these rates, the magnitude of $a – b$ is comparable to typical published values for fault gouges, which vary from –0.001 to –0.01 (for example, Blanpied and others, 1987; Kilgore and others, 1993). Above 10^{-4} m/s and at the lowest normal stresses of these experiments, $a – b$ is positive, indicating that the gouge is rate strengthening. The apparent transition from negative to positive values of $a – b$ occurs at a shear rate similar to the same transition documented for other rock and gouge shear zones (for example, Shimamoto, 1986; Blanpied and others, 1987; Kilgore and others, 1993).

The transition shear rate in our experiments is only moderately larger than the rate of extrusion estimated for much of the 2004–2005 eruption (3×10^{-5} m/s to 7×10^{-5} m/s), but two observations indicate that gouge shear rates at Mount St. Helens may be well within the rate-weakening regime. Kilgore

and others (1993) noted that the transition shear rate increases with increasing normal stress. Because normal stresses in our experiments were probably at least one order of magnitude smaller than those on the margins of the magma plug at depths of 100–500 m at Mount St. Helens (2–10 MPa), rate-weakening behavior at Mount St. Helens would likely be exhibited at higher shear rates than those of the experiments. Secondly, Marone and Kilgore (1993) showed that the characteristic slip distance D_c is more appropriately viewed as a characteristic shear strain (shear displacement divided by the shear-zone thickness) when considering shear within a gouge layer. In ring-shear experiments on the Mount St. Helens gouge in which we placed vertical columns of beads in the gouge to study the shear-strain distribution, more than 90 percent of the strain was distributed over a thickness of 10 mm. At Mount St. Helens, the shear-zone thickness is likely larger, given the ~1 m total thickness of the gouge layer and presence of particles too large to include in the ring-shear experiments. Thus, shear-strain rates in the ring-shear experiments were likely larger at a particular shear rate than those at Mount St. Helens, indicating that the gouge there would likely rate-weaken at higher shear rates than it did in the experiments. Thus, one of the conditions required for stick-slip ascent of the dacite plug—rate weakening of the gouge—appears to be met.

Table 1. Rate-dependence parameters.

[Value *a–b* describes sign and magnitude of rate dependence of gouge friction. The *b* value alone describes magnitude of gouge strengthening as a function of hold time.]

Normal stress (kPa)	Shear-rate range (m/s)	*a–b*	*b*
Fast			
5	5×10^{-4} – 5×10^{-3}	0.0150	
23	5×10^{-4} – 5×10^{-3}	0.0105	
Slow			
5	1.5×10^{-6} – 2.5×10^{-5}	–0.0250	
23	1.5×10^{-6} – 2.5×10^{-5}	0.00099	
86	1.5×10^{-6} – 2.5×10^{-5}	–0.0022	
141	1.5×10^{-6} – 2.5×10^{-5}	–0.0013	
159	1.5×10^{-6} – 2.5×10^{-5}	–0.0024	0.0079
195	1.5×10^{-6} – 2.5×10^{-5}	–0.0103	

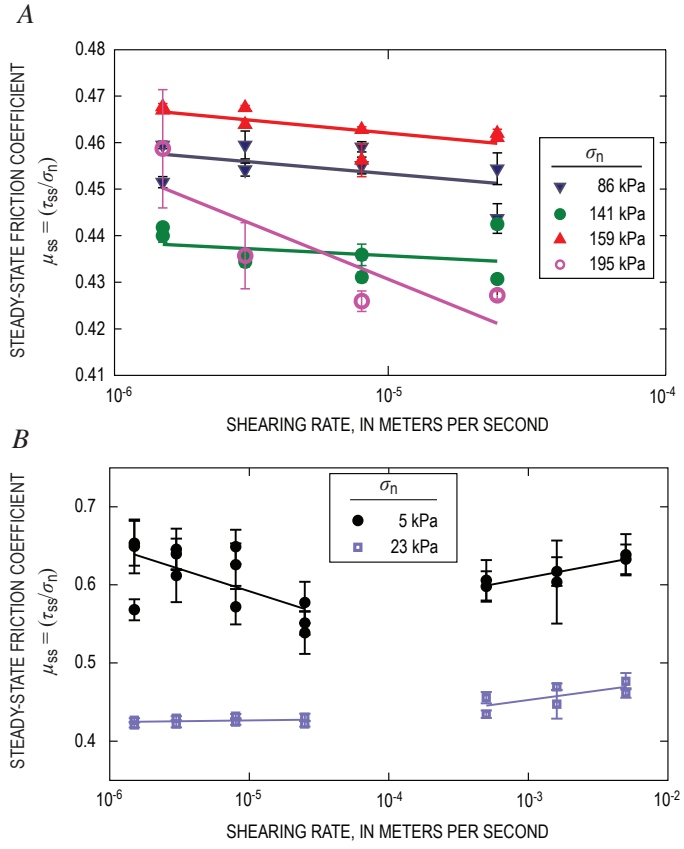

Figure 5. Steady-state friction coefficient as a function of shear rate. Each data point represents results of one experiment. Steady-state friction coefficient is shear stress supported by the gouge divided by corrected normal stress, both averaged over the part of experiment when time-averaged steady state had been attained (see fig. 4). Data are grouped by magnitude of applied normal stress. Error bars represent ±1 standard deviation of observed variability in friction coefficient during the period of the time-averaged steady state. *A*, High applied normal stresses. *B*, Low applied normal stresses.

We now consider the second condition—that the stiffness of the loading system must be smaller than the critical stiffness defined by the evolution behavior of the gouge. Assessment of this condition requires independent estimates of both the in situ critical stiffness k_{crit} of the gouge and the stiffness k_{sys} of the magma that is driving extrusion.

The critical stiffness of the gouge was defined by Ruina (1983) as the post-peak reduction in shear stress divided by the characteristic slip distance over which this reduction occurs:

$$k_{crit} = \frac{-(a-b)\sigma_n'}{D_c}, \qquad \text{for } (a-b) < 0. \tag{6}$$

If a lithostatic stress state is assumed at the nucleation depth of the drumbeat earthquakes (~500 m) and pore-water pressure is neglected, such that the total normal stress equals the effective normal stress, then σ_n' ~10 MPa. A reasonable value of *a–b* indicated by our experimental results is –0.003. The characteristic slip distance D_c can be determined from the transition from steady slip to persistent stick-slip behavior that occurred in our experiments with high normal stresses. At this transition the experimental normal stress was 195 kPa (table 1), and k_{crit} equaled the stiffness of the test device. This stiffness is approximately 1.7×10^4 kPa/m (see appendix 1). (Here, again following Ruina (1983), we employ a stiffness having dimensions of stress per unit length (that is, mass/(time^2×length^2))). Substituting this value for k_{crit}, *a–b* = –0.003 and the experimental value of σ_n' (195 kPa) in equation 6 yields D_c = 34 µm, which is of the same order as typical laboratory values for gouge (for example, Marone and Kilgore, 1993). Assuming that D_c = 34 µm, *a–b* = –0.003, and σ_n' =10 MPa are appropri-

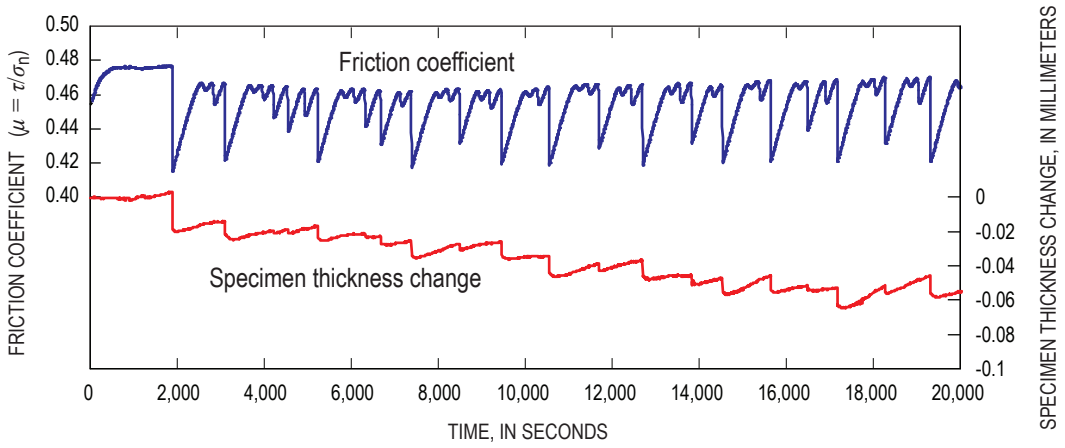

Figure 6. Part of one record of stick slip from experiments conducted at the two lowest shear rates (1.5×10^{-6} and 3.0×10^{-6} m/s) at 195 kPa normal stress. No direct measurement was made of displacement of the rotating base during these tests, so stick-slip displacement was inferred from shear-stress and specimen thickness records.

ate for the in situ gouge at Mount St. Helens, then equation 6 yields an in situ critical gouge stiffness of ~10^6 kPa/m.

To estimate the stiffness of the loading system, we assume that magma underlying the plug drives extrusion (fig. 8), and that the magma contains about 12 percent exsolved gas by volume (T. Gerlach, oral commun., 2005) and has a compressibility $\alpha = 10^{-4}$ per kPa (Iverson, this volume, chap. 21). The pertinent stiffness k is the magmatic "spring force" per unit area of plug-margin slip surface divided by the "spring displacement" associated with magma compression-relaxation cycles (compare with Ruina, 1983). To estimate this k, we approximate the magma body as a right circular column with height H = 8,000 m and cross sectional area $A=1/4(\pi d^2)$, where d is the mean column diameter, and we approximate the area of the slip surface on the margins of the plug as πdh, where h is the height of the plug in contact with the conduit walls. The spring force associated with magma compression is $(A/\alpha)(\delta/H)$, where δ is the characteristic displacement associated with magma compression or relaxation, and δ/H is the accompanying longitudinal strain of the magma column. Thus, the spring force per unit area of slip surface is $d\delta/(4\alpha hH)$, and dividing this expression by the displacement distance δ yields

$$k = d/(4\alpha hH). \qquad (7)$$

If h is 500 m, and d is 50 m (these values are probably of the correct order of magnitude for the geometry at Mount St. Helens), then inserting these values and the α and H values noted above into equation 7 yields k ~10^{-1} kPa/m, seven orders of magnitude smaller than the critical gouge stiffness k_{crit} ~10^6 kPa/m. Therefore, even if the estimated values of magma compressibility or the geometrical parameters d, h, and H are greatly in error, the gouge is likely much stiffer than the magma column that drives upward movement of the plug. Thus, in addition to rate weakening of the gouge, the second requirement for stick-slip—that the critical stiffness of the gouge exceeds the stiffness of some part of the loading system—is likely satisfied.

The finding that the magma-plug system can exhibit stick-slip behavior at shallow depths contrasts with the common observation that fault slip is aseismic within ~2 km of the surface (Scholz, 2002). The tendency for aseismic tectonic fault slip at shallow depths is commonly attributed either to rate strengthening in unconsolidated gouge or to the dependence of critical stiffness on normal stress, which is low near Earth's surface (Marone and Scholz, 1988; Scholz, 2002). Our results indicate that the Mount St. Helens gouge is rate weakening and the loading-system stiffness is exceptionally small owing to the presence of a large body of highly compressible magma. Therefore, stick-slip behavior should be possible at much smaller depths at Mount St. Helens than would be predicted for tectonically driven crustal faults.

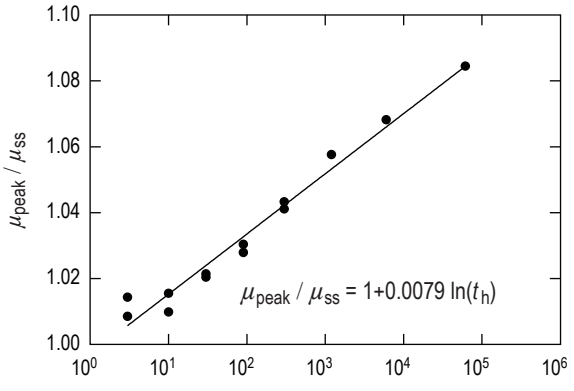

Figure 7. Normalized peak friction coefficient, μ_{peak}, as a function of logarithm of hold time. Standard error of b-value (slope of the regression) is 0.0004. All tests were at a normal stress of 159 kPa and shear rate of 2.5×10^{-5} m/s.

Conclusions

Under normal stresses less than about 200 kPa, gouge sampled from the surface of the newly extruded Mount St. Helens dome in February 2005 exhibits frictional behavior that is described well by the rate- and state-dependent friction model. In our ring-shear device the gouge weakens with increasing steady shear rates up to about 10^{-4} m/s and strengthens at larger shear rates. This transition from weakening to strengthening occurs at an experimental shear rate only moderately larger than the observed time-averaged rate of extrusion at Mount St. Helens, but in situ the transition probably occurs at higher shear rates because in situ normal stresses in the gouge are probably significantly larger than those that could be applied experimentally. Also, the in situ stiffness of the gouge, as estimated using the conditions under which stick-slip occurred in the experiments, is roughly seven orders of magnitude greater than the stiffness of the most compliant component of the system driving uplift of the plug: the underlying magma. The rate weakening and high stiffness of the gouge relative to the magma are requirements for stick-slip behavior when rate-and-state dependent friction is present, so stick-slip behavior provides a viable hypothesis for the source of the observed shallow drumbeat earthquakes at Mount St. Helens. In addition, experiments showed that the peak strength of the gouge increased logarithmically with hold time, indicating that deformation history of the gouge could influence the character of stick-slip behavior and associated seismicity.

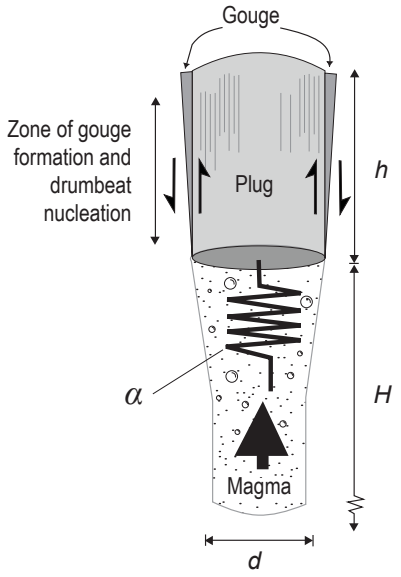

Figure 8. Schematic illustration of hypothesized magma-plug system at Mount St. Helens. Cool, rigid dacite plug is driven upward through upper conduit by ascending compressible magma. Gouge forms by frictional wear at interface between extruding plug and conduit. Because the gouge is stiffer than effective stiffness of the magma that is driving plug uplift, uplift occurs in stick-slip cycles, producing drumbeat earthquakes. Physical and geometrical variables (letters and symbols on figure) are discussed in text.

Acknowledgments

We thank John Pallister for collection of gouge samples from Mount St. Helens. Technical reviews by Nick Beeler and John Power and editorial suggestions by Jim Hendley significantly improved this paper.

References Cited

Beeler, N.M., Tullis, T.E., and Weeks, J.D., 1994, The roles of time and displacement in the evolution effect in rock friction: Geophysical Research Letters, v. 21, no. 18, p. 1987–1990.

Biegel, R.L., Sammis, C.G., and Dieterich, J.H., 1989, The frictional properties of a simulated gouge having a fractal particle distribution: Journal of Structural Geology, v. 11, no 7, p. 827–846.

Blanpied, M.L., Tullis, T.E., and Weeks, J.D., 1987, Frictional behavior of granite at low and high sliding velocities: Geophysical Research Letters, v. 15, no. 5, p. 554–557.

Dieterich, J.H., 1972, Time dependence of rock friction: Journal of Geophysical Research, v. 77, p. 3690–3697.

Dieterich, J.H., 1978, Time dependent friction and the mechanics of stick-slip: Pure and Applied Geophysics, v. 116, p. 790–806.

Dieterich, J.H., 1979, Modeling of rock friction 1—experimental results and constitutive equations: Journal of Geophysical Research, v. 84, no. B5, p. 2161–2168.

Engelder, J.T., 1974, Cataclasis and the generation of fault gouge: Geological Society of America Bulletin, v. 85, p. 1515–1522.

Head, K.H., 1989, Soil technician's handbook: New York, John Wiley, 83 p.

Hooyer, T.S., and Iverson, N.R., 2000, Clast-fabric development in a shearing granular material—implications for subglacial till and fault gouge: Geological Society of America Bulletin, v. 112, no. 5, p. 683–692.

Iverson, R.M., 2008, Dynamics of seismogenic volcanic extrusion resisted by a solid surface plug, Mount St. Helens, 2004–2005, chap. 21 *of* Sherrod, D.R., Scott, W.E., and Stauffer, P.H., eds., A volcano rekindled; the renewed

eruption of Mount St. Helens, 2004–2006: U.S. Geological Survey Professional Paper 1750 (this volume).

Iverson, N.R., Baker, R.W., and Hooyer, T.S., 1997, A ring-shear device for the study of till deformation—tests on tills with contrasting clay contents: Quaternary Science Reviews, v. 16, no. 9, p. 1057–1066.

Iverson, N.R., Hooyer, T.S., and Baker, R.W., 1998, Ring-shear studies of till deformation—Coulomb-plastic behavior and distributed strain in glacier beds: Journal of Glaciology, v. 16, p. 1057–1066.

Iverson, R.M., Reid, M.E., Iverson, N.R., LaHusen, R.G., Logan, M., Mann, J.E., and Brien, D.L., 2000, Acute sensitivity of landslide rates to initial porosity: Science, v. 290, p. 513–516.

Iverson, R.M., Dzurisin, D., Gardner, C.A., Gerlach, T.M., LaHusen, R.G., Lisowski, M., Major, J.J., Malone, S.D., Messerich, J.A., Moran, S.C., Pallister, J.S., Qamar, A.I., Schilling, S.P., and Vallance, J.W., 2006, Dynamics of seismogenic volcanic extrusion at Mount St. Helens in 2004–05: Nature, v. 444, no. 7118, p. 439–443, doi:10.1038/nature05322.

Kilgore, B.D., Blanpied, M.L., and Dieterich, J.H., 1993, Velocity dependent friction of granite over a wide range of conditions: Geophysical Research Letters, v. 20, no. 10, p. 903–906.

Lambe, T.W., and Whitman, R.V., 1969, Soil Mechanics: New York, John Wiley, 553 p.

Losert, W., Géminard, J.-C., Nasuno, S., and Gollub, J.P., 2000, Mechanisms for slow strengthening in granular materials: Physical Review E, v. 61, no. 4, p. 4060–4068.

Marone, C., 1998, Laboratory-derived friction laws and their application to seismic faulting: Annual Reviews of Earth and Planetary Science, v. 26, p. 643–696.

Marone, C., and Kilgore, B., 1993, Scaling of the critical slip distance for seismic faulting with shear strain in fault zones: Nature, v. 362, p. 618–620.

Marone, C., and Scholz, C.H., 1988, The depth of seismic faulting and the upper transition from stable to unstable slip regimes: Geophysical Research Letters, v. 15, no. 6, p. 621–624.

Marone, C., Raleigh, C.B., and Scholz, C.H., 1990, Frictional behavior and constitutive modeling of simulated fault gouge: Journal of Geophysical Research, v. 95, no. B5, p. 7007–7025.

Moore, P.L., and Iverson, N.R., 2002, Slow episodic shear of granular materials regulated by dilatant strengthening: Geology, v. 30, p. 843–846.

Rice, J.R., and Ruina, A., 1983, Stability of steady frictional slipping: Journal of Applied Mechanics, v. 50, p. 343–349.

Ruina, A., 1983, Slip instability and state variable friction laws: Journal of Geophysical Research, v. 88, no. B12, p. 10359–10370.

Scherer, R.P., Sjunneskog, C.M., Iverson, N.R., and Hooyer, T.S., 2004, Assessing subglacial processes from diatom fragmentation patterns: Geology, v. 32, p. 557–560.

Scholz, C.H., 2002, Mechanics of earthquakes and faulting (2d ed.): New York, Cambridge University Press, 471 p.

Shimamoto, T., 1986, Transition between frictional slip and ductile flow for halite shear zones at room temperature: Science, v. 231, p. 711–714.

Tuffen, H., and Dingwell, D., 2005, Fault textures in volcanic conduits; evidence for seismic trigger mechanisms during silicic eruptions: Bulletin of Volcanology, v. 67, p. 370–387.

Appendix 1. Stiffness of the Ring-Shear Device

The stiffness of the ring-shear device can be estimated from stress-displacement transients that were common when shearing was initiated in experiments conducted at the highest normal stresses. Particularly after extended hold periods, the start of shear was characterized by sudden stress reductions that accompanied abrupt slip (fig. 9). Abrupt slip displacement was measured with a horizontally oriented LVDT that pressed on an armature extending from the rotating base of the device. This abrupt displacement of the rotating base occurred despite the constant speed of the motor driving the rotation of the base. These events reflect the release of elastic strain energy stored in the drive mechanism of the device, and therefore the ratio of abrupt stress reduction to abrupt slip describes the device stiffness, as applicable to the rate-and-state model of Ruina (1983)—1.7×10^4 kPa/m.

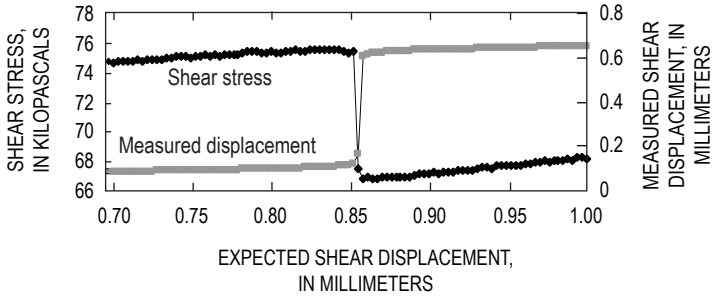

Figure 9. Shear stress and measured shear displacement during initial minutes of a ring-shear test conducted at a normal stress of 159 kPa. Data are plotted as a function of expected shear displacement calculated from rotation rate of motor that drives rotating base (fig. 3). Data begin when motor was actively driving rotation, but no displacement was measured at perimeter of the rotating base. During subsequent abrupt slip, there was a marked reduction in measured shear stress, well below steady-state strength of the gouge. This stress reduction and associated abrupt displacement are interpreted to reflect elastic compliance of the device.